Transp Porous Med (2012) 91:261–279
DOI 10.1007/s11242-011-9843-5

Radiation Effects on Mixed Convection over a Wedge Embedded in a Porous Medium Filled with a Nanofluid

Ali J. Chamkha · S. Abbasbandy · A. M. Rashad · K. Vajravelu

Received: 29 April 2011 / Accepted: 25 August 2011 / Published online: 16 September 2011

Abstract The problem of steady, laminar, mixed convection boundary-layer flow over an isothermal vertical wedge embedded in a porous medium saturated with a nanofluid is studied, in the presence of thermal radiation. The model used for the nanofluid incorporates the effects of Brownian motion and thermophoresis with Rosseland diffusion approximation. The wedge surface is maintained at a constant temperature and a constant nanoparticle volume fraction. The resulting governing equations are non-dimensionalized and transformed into a non-similar form and then solved by Keller box method. A comparison is made with the available results in the literature, and our results are in very good agreement with the known results. A parametric study of the physical parameters is made, and a representative set of numerical results for the velocity, temperature, and volume fraction, the local Nusselt and Sherwood numbers are presented graphically. The salient features of the results are analyzed and discussed.

Keywords Mixed convection · Porous media · Nanofluid · Wedge · Thermophoresis · Brownian diffusion · Thermal radiation · Keller box method

A. J. Chamkha
Manufacturing Engineering Department, The Public Authority for Applied Education and Training, 70654 Shuweikh, Kuwait

S. Abbasbandy (✉)
Department of Mathematics, Imam Khomeini International University, 34194 Ghazvin, Iran
e-mail: abbasbandy@yahoo.com

A. M. Rashad
Department of Mathematics, South Valley University, Faculty of Science, Aswan, 81528, Egypt

K. Vajravelu
Department of Mathematics, University of Central Florida, Orlando, FL 32816, USA

1 Introduction

Fluid flow and heat transfer in porous media received considerable interest during the last several decades. This is primarily because of the numerous applications of flow through porous medium, such as storage of radioactive nuclear waste, transpiration cooling, separation processes in chemical industries, filtration, transport processes in aquifers, groundwater pollution, geothermal extraction and fiber insulation. Theories and experiments of thermal convection in porous media and state-of-the-art reviews with special emphasis on practical applications are presented in the recent books by Nield and Bejan (2006), Pop and Ingham (2001), Ingham and Pop (2002), Bejan et al. (2004) and Vafai (2005).

Nanofluid is envisioned to describe a fluid, in which nanometer-sized particles are suspended, in convectional heat transfer of basic fluids. Convectional heat transfer fluids, including oil, water and ethylene glycol mixture, are poor heat transfer fluids, since the thermal conductivity of these fluids plays important role on the heat transfer coefficient between the heat transfer medium and the heat transfer surface. Therefore, numerous methods are proposed to improve the thermal conductivity of these fluids by suspending nano/micro-sized particle materials in liquids. Recently, several numerical studies on the modeling of natural convection heat transfer in nanofluids are published. The term nanofluid refers to these kinds of fluids by suspending nanoscale particles in the base fluid, and the idea is introduced by Choi (1995). Duangthongsuk and Wongwises (2008) studied the influence of thermophysical properties of nanofluids on the convective heat transfer and summarized various models used in the literature for predicting the thermophysical properties of nanofluids. The problem of the thermal instability in a porous medium layer saturated by a nanofluid was investigated by Nield and Kuznetsov (2009). Abu-Nada and Oztop (2009) studied the effects of inclination angle on natural convection in enclosures filled with Cu-water nanofluid. Nield and Kuznetsov (2009) suggested natural convective boundary-layer flow of a nanofluid past a vertical plate. Chamkha et al. (2011) studied the mixed convection MHD flow of a nanofluid past a stretching permeable surface in the presence of Brownian motion and thermophoresis effects. Also, Chamkha et al. (2011) analyzed the natural convection flow past a sphere embedded in a porous medium saturated by a nanofluid. Gorla et al. (2011a,b) studied the steady boundary-layer flow of a nanofluid on a stretching circular cylinder in a stagnant free stream. Furthermore, Gorla et al. (2011a,b) analyzed the problems of mixed convection past a vertical wedge embedded in a porous medium saturated by a nanofluid and the heat transfer in the boundary layer on a stretching circular cylinder in a nanofluid, respectively.

However, the thermal radiation effect on mixed convection heat transfer in porous media is very important in high-temperature processes and space technology and has many important applications such as space technology, and processes involving high temperatures such as geothermal engineering, the sensible heat storage bed, the nuclear reactor cooling system and underground nuclear wastes disposal. Yih (1999, 2001) studied radiation effect on mixed convection over an isothermal wedge/cone in porous media. Bakier (2001) presented an analysis of the thermal radiation effect on stationary mixed convection from vertical surfaces in saturated porous media. Kumari and Nath (2004) studied the radiation effect on the non-Darcy mixed convection flow over a non-isothermal horizontal surface in a porous medium. Chamkha and Ben-Nakhi (2008) studied the mixed convection–radiation interaction along a permeable surface immersed in a porous medium. The problem of hydromagnetic heat transfer by mixed convection from melting of a vertical plate in a liquid-saturated porous medium, taking into account the effects of thermal radiation, was investigated by Bakier et al. (2009). Also, the study of convection heat transfer from a cone/wedge is of special interest and has wide range of practical applications. Mainly, these types of heat transfer

problems deal with the design of spacecrafts, nuclear reactors, solar power collectors, power transformers, steam generators and others. Many investigations (Pop et al. 2003; Takhar et al. 2004; Alam et al. 2007; Vajravelu and Nayfeh 1992) have developed similarity and non-similarity solutions for natural convection flows over a vertical cone/wedge in steady state.

Motivated by these studies, the problem of steady, laminar, mixed convection boundary-layer flow over an isothermal vertical wedge embedded in a porous medium saturated with a nanofluid, in the presence of thermal radiation, is studied. The model used for the nanofluid incorporates the effects of Brownian motion and thermophoresis with Rosseland diffusion approximation. The resulting governing equations are non-dimensionalized and transformed into a non-similar form and then solved by Keller box method. A comparison is made with the available results in the literature, and the salient features of the new results are analyzed and discussed.

2 Problem Formulation

Consider the problem of the radiation effect on mixed convection boundary-layer flow of optically dense viscous incompressible nanofluid over an isothermal wedge embedded in a saturated porous medium. The model used for the nanofluid incorporates the effects of Brownian motion and thermophoresis. The uniform wall temperature of the wedge T_w and uniform nanoparticle volume fraction C_w are higher than the ambient temperature T_∞ and ambient nanoparticle volume fraction C_∞, respectively. The flow over the wedge is assumed to be two-dimensional, laminar, steady and incompressible (see Fig. 1 for the flow model and the physical coordinate system). The porous medium is assumed to be uniform and isotropic and is in local thermal equilibrium with the fluid. All fluid properties are assumed to be constant. Under the Boussinesq and the Rosseland diffusion approximations, the governing equations based on the Darcy law proposed by Hsieh et al. (1993) and Yih (2001) can be written as

$$\frac{\partial u}{\partial x} + \frac{\partial v}{\partial y} = 0, \tag{1}$$

$$\frac{\partial u}{\partial y} = \frac{(1 - C_\infty)\,\rho_{f\infty}\beta g K}{\mu}\frac{\partial T}{\partial y} - \frac{\left(\rho_p - \rho_{f\infty}\right) g K}{\mu}\frac{\partial C}{\partial y}, \tag{2}$$

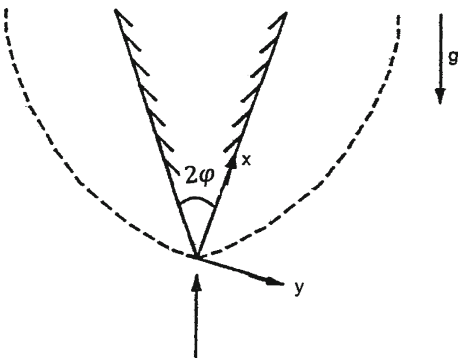

Fig. 1 Flow model and coordinate system

$$u\frac{\partial T}{\partial x}+v\frac{\partial T}{\partial y}=\alpha_e\frac{\partial^2 T}{\partial y^2}+\tau\left[D_{\mathrm{B}}\frac{\partial C}{\partial y}\frac{\partial T}{\partial y}+\left(\frac{D_{\mathrm{T}}}{T_\infty}\right)\left(\frac{\partial T}{\partial y}\right)^2\right]+\frac{16\sigma}{3(a_r+\sigma_s)(c_p\rho)_f}\frac{\partial}{\partial y}\left(T^3\frac{\partial T}{\partial y}\right), \tag{3}$$

$$u\frac{\partial C}{\partial x}+v\frac{\partial C}{\partial y}=D_{\mathrm{B}}\frac{\partial^2 C}{\partial y^2}+\left(\frac{D_{\mathrm{T}}}{T_\infty}\right)\frac{\partial^2 T}{\partial y^2}, \tag{4}$$

where x and y denote the vertical and horizontal directions, respectively. u, v, T and C are the x and y components of velocity, temperature and nanoparticle volume fraction, respectively. K, β, D_{B} and D_{T} are the permeability of the porous medium, volumetric expansion coefficient of fluid, the Brownian diffusion coefficient and thermophoretic diffusion coefficient, respectively. μ, ρ_f and ρ_p are the fluid viscosity, fluid density and the nanoparticle mass density, respectively. g, σ, σ_s and a_r are the acceleration due to gravity, the Stefan–Boltzmann constant, scattering coefficient and the Rosseland mean extinction coefficient, respectively. $\alpha_{\mathrm{e}}=k/(\rho c)_f$ and $\tau=(\rho c)_p/(\rho c)_f$ are the thermal diffusivity of porous medium and the ratio of heat capacities, respectively. k, $(\rho c)_f$ and $(\rho c)_p$ are thermal conductivity, heat capacity of the fluid and the effective heat capacity of nanoparticle material, respectively. The last term on the right side of the energy Eq. 3 is the thermal radiation heat flux and is approximated using the Roseland diffusion equation.

The appropriate boundary conditions suggested by the physics of the problem are

$$y=0:\quad v(x,0)=0,\quad T=T_{\mathrm{w}},\quad C=C_{\mathrm{w}}, \tag{5a}$$

$$y\to\infty:\quad u=U_\infty,\quad T=T_\infty,\quad C=C_\infty, \tag{5b}$$

where T_{w} and C_{w} are the wall temperature and wall nanoparticle volume fraction, respectively. U_∞, T_∞ and C_∞ are the free stream velocity, temperature and nanoparticle volume fraction, respectively. It is convenient to transform the governing equations into a non-similar dimensionless form that can be studied as an initial-value problem. This can be done by introducing the stream function: $u=\partial\psi/\partial y$, $v=-\partial\psi/\partial x$ and using

$$\begin{aligned}
&\eta=\frac{y}{x}\left(Pe_x^{1/2}\right)\chi^{-1},\ \chi=\left(1+\left(\frac{Ra_x}{Pe_x}\right)^{1/2}\right)^{-1}\\
&\psi=\alpha_e\left(Pe_x^{1/2}\right)\chi^{-1}f(\chi,\eta),\ \theta=\frac{T-T_\infty}{T_{\mathrm{w}}-T_\infty},\\
&\phi=\frac{C-C_\infty}{C_{\mathrm{w}}-C_\infty},\quad \lambda=\frac{\varphi}{\pi-\varphi},\quad U_\infty=Bx^{\lambda},\quad Pe_x=U_\infty x/\alpha_e,\\
&Ra_x=\left\{(1-C_\infty)\,\rho_{f\infty}g\,\beta_T K\,(T_{\mathrm{w}}-T_\infty)\,x/\mu\alpha_e\right\},
\end{aligned} \tag{6}$$

where Pe_x and Ra_x are the local Peclet and modified Rayleigh numbers, respectively. The parameters a, φ and λ are the free stream velocity constant, half-wedge angle and the free stream velocity exponent, respectively. Using the expressions in (6), we can write Eqs. 1–5 as

$$f''=(1-\chi)^2\left(\theta'-Nr\phi'\right), \tag{7}$$

$$\theta'' + \frac{1}{2}(1+\lambda\chi) f\theta' + N\mathrm{b}\phi'\theta' + N\mathrm{t}\theta'^2 + \frac{4R_\mathrm{d}}{3}\left\{\theta'\left[(H-1)\theta+1\right]^3\right\}' = \frac{\lambda}{2}\chi(1-\chi)\left(f'\frac{\partial\theta}{\partial\chi} - \theta'\frac{\partial f}{\partial\chi}\right), \tag{8}$$

$$\phi'' + \frac{Le}{2}(1+\lambda\chi) f\phi' + \frac{N\mathrm{t}}{N\mathrm{b}}\theta'' = \frac{Le}{2}\lambda\chi(1-\chi)\left(f'\frac{\partial\phi}{\partial\chi} - \phi'\frac{\partial f}{\partial\chi}\right), \tag{9}$$

$$(1+\lambda\chi) f(\chi,0) - \lambda\chi(1-\chi)\frac{\partial f}{\partial\chi}(\chi,0) = 0, \quad \theta(\chi,0) = 1, \quad \phi(\chi,0) = 1, \tag{10a}$$

$$f'(\chi,\infty) = \chi^2, \quad \theta(\chi,\infty) = 0, \quad \phi(\chi,\infty) = 0, \tag{10b}$$

where $Le = \frac{\alpha_e}{D_\mathrm{B}}$, $N\mathrm{r} = \frac{(\rho_p-\rho_{f\infty})(C_\mathrm{w}-C_\infty)}{(1-C_\infty)\rho_{f\infty}\beta(T_\mathrm{w}-T_\infty)}$, $N\mathrm{b} = \frac{\varepsilon(\rho c)_p D_\mathrm{B}(C_\mathrm{w}-C_\infty)}{(\rho c)_f\alpha_e}$,

$$N\mathrm{t} = \frac{\varepsilon(\rho c)_p D_\mathrm{T}(T_\mathrm{w}-T_\infty)}{(\rho c)_f\alpha_e T_\infty}, \quad R_\mathrm{d} = 4\sigma T_\infty^3/\left[k(a_r+\sigma_s)\right], \quad H = T_\mathrm{w}/T_\infty, \tag{11}$$

are the Lewis number, buoyancy ratio, Brownian motion parameter, thermophoresis parameter, mixed convection parameter, conduction–radiation parameter and the surface temperature excess ratio, respectively. It should be noted that $\chi = 0\,(Pe_x = 0)$ corresponds to pure free convection while $\chi = 1(Ra_x = 0)$ corresponds to pure forced convection. The entire regime of mixed convection corresponds to the values of χ between 0 and 1.

Of special significance for this problem are the local Nusselt and Sherwood numbers. These physical quantities can be defined as

$$\frac{Nu_x}{Ra_x^{1/2} + Pe_x^{1/2}} = -\theta'(\chi,0)\left(1 + \frac{4R_\mathrm{d}H^3}{3}\right), \tag{12}$$

$$\frac{Sh_x}{Ra_x^{1/2} + Pe_x^{1/2}} = -\varphi'(\chi,0). \tag{13}$$

Table 1 Comparison of values of $-\theta'(\xi,0)$ for various values of λ and χ in the absence of nanoparticles volume fraction, Brownian motion and thermophoresis effects ($N\mathrm{r} = N\mathrm{b} = N\mathrm{t} = 0$)

	Hsieh et al. (1993)	Yih (2001)			Present results		
χ	$\lambda = 0$	$\lambda = 0$	$\lambda = 1/3$	$\lambda = 1$	$\lambda = 0$	$\lambda = 1/3$	$\lambda = 1$
1.0	0.5642	0.5642	0.6515	0.7979	0.5642	0.6516	0.7979
0.9	0.5098	0.5097	0.5878	0.7181	0.5098	0.5879	0.7181
0.8	0.4603	0.4602	0.5278	0.6385	0.4602	0.5280	0.6385
0.7	0.4174	0.4173	0.4731	0.5599	0.4173	0.4732	0.5599
0.6	0.3832	0.3832	0.4261	0.4854	0.3832	0.4261	0.4854
0.5	0.3603	0.3603	0.3900	0.4227	0.3603	0.3901	0.4227
0.4	0.3506	0.3505	0.3686	0.3823	0.3506	0.3687	0.3823
0.3	0.3550	0.3550	0.3643	0.3697	0.3550	0.3643	0.3697
0.2	0.3732	0.3732	0.3769	0.3786	0.3732	0.3769	0.3786
0.1	0.4035	0.4035	0.4044	0.4049	0.4035	0.4043	0.4049
0.0	0.4438	0.4437	0.4437	0.4437	0.4437	0.4437	0.4437

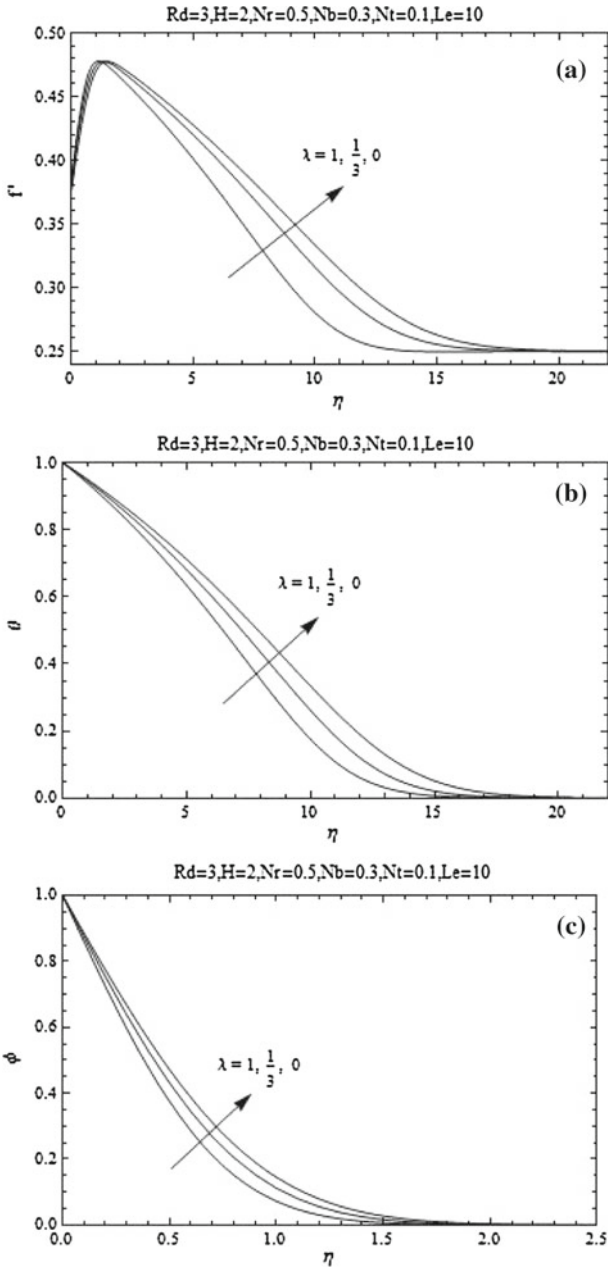

Fig. 2 **a** Effect of λ on the velocity profiles. **b** Effect of λ on the temperature profiles. **c** Effect of λ on the volume fraction profiles

3 Numerical Method and Validation

The governing Eqs. 7, 8 and 9 with the boundary conditions (10) are non-linear partial differential equations. Hence, the system of Eqs. 7–9 is solved numerically using an implicit finite

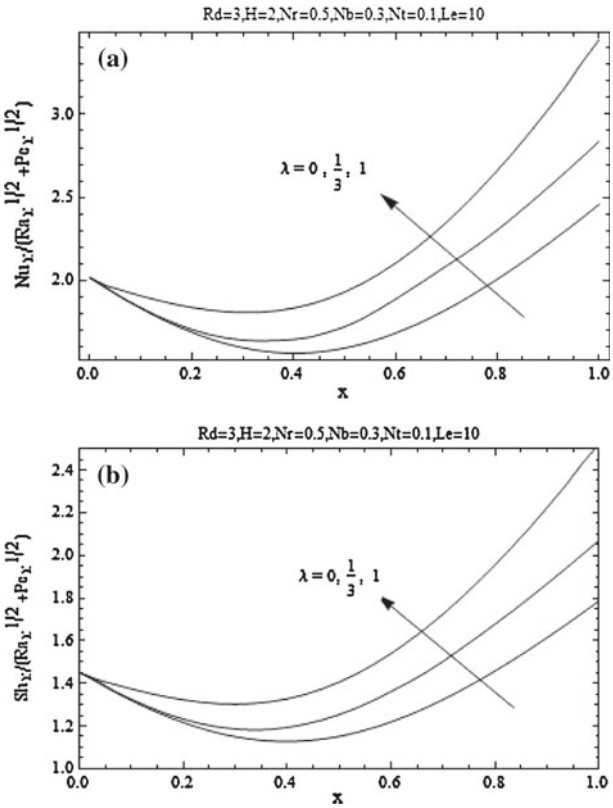

Fig. 3 **a** Effect of λ on the local Nusselt number. **b** Effect of λ on the local Sherwood number

difference scheme known as the Keller box method as described by Cebeci and Bradshaw (1984). The computations were carried out with $\Delta\chi = 0.01$ and $\Delta\eta = 0.01$ (uniform grids). The value of $\eta_\infty = 50$ is found to be sufficiently enough to obtain the accuracy of $|\theta'(0)| < 10^{-5}$.

In order to validate the numerical results, comparisons with the previously published results of Hsieh et al. (1993) and Yih (2001) for the case of Newtonian fluid are made when $R_d = Nr = Nb = Nt = 0$. These comparisons are presented in Table 1. It is easy to see from the table that an excellent agreement exists between the results.

4 Results and Discussion

In this section, representative numerical results are displayed with the help of graphical illustrations. Computations were carried out for various values of physical parameters such as the wedge angle parameter λ, buoyancy ratio Nr, the Brownian motion parameter Nb, thermophoresis parameter Nt, surface temperature parameter H, radiation–conduction parameter R_d, the Lewis number Le and the mixed convection parameter χ.

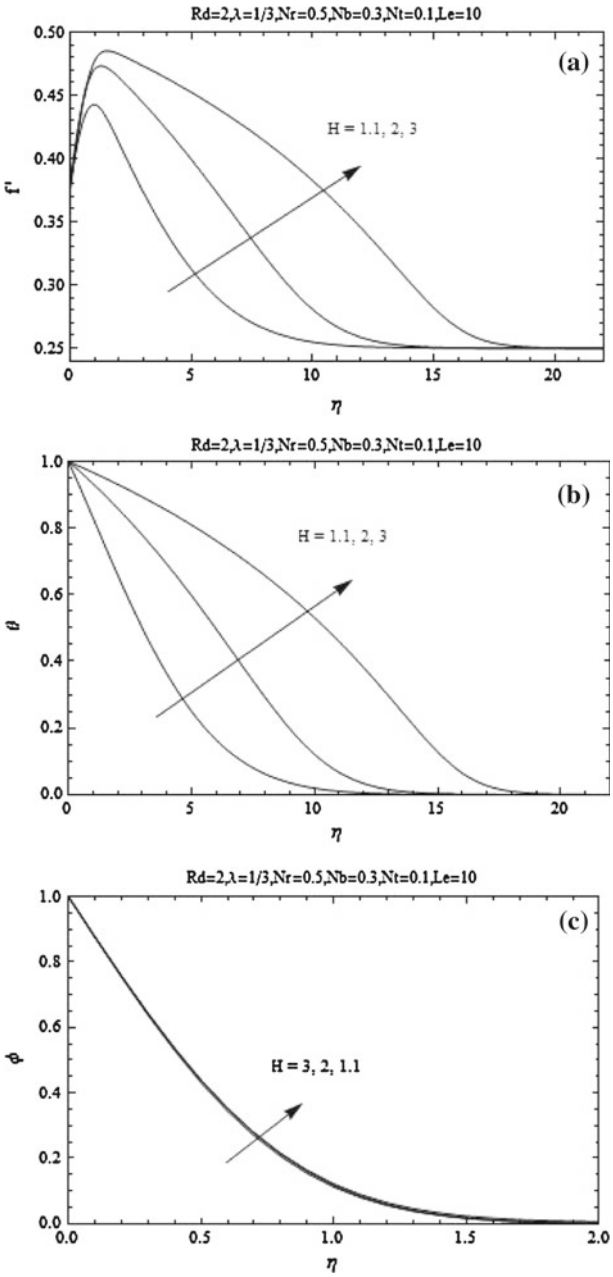

Fig. 4 **a** Effect of H on the velocity profiles. **b** Effect of H on the temperature profiles. **c** Effect of H on the volume fraction profiles

Figure 2a–c show representatively the velocity f', the temperature θ and the nanoparticles volume fraction ϕ profiles for different values of the wedge angle parameter λ. It is clear that the fluid velocity, the temperature and the volume fraction decrease while the negative

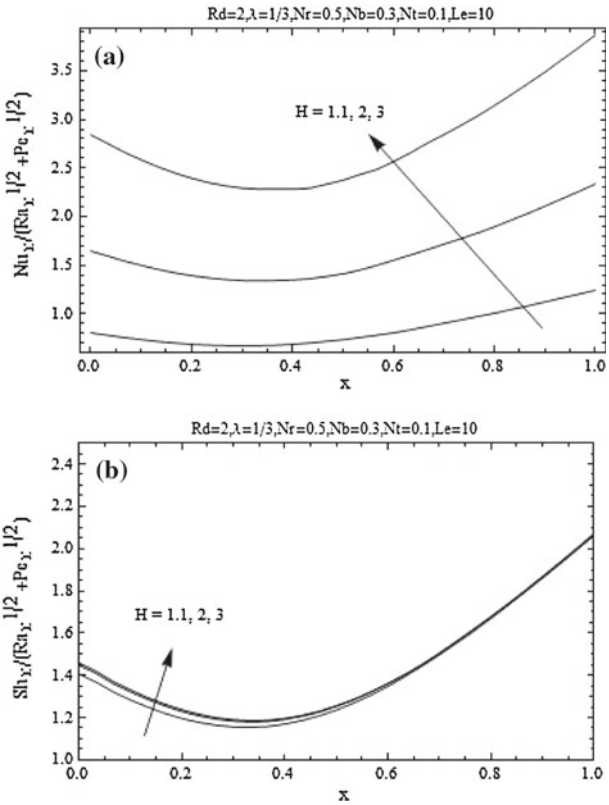

Fig. 5 **a** Effect of H on the local Nusselt number. **b** Effect of H on the local Sherwood number

values of their wall slopes increase as λ increases. This has the enhancing effect on both heat and mass transfer.

In Fig. 3a–c, we present, respectively, the effects of the wedge angle parameter λ on the local Nusselt number $-\left(1+(4R_{\mathrm{d}}H^3/3)\right)\theta'(\chi,0)$ and on the local Sherwood number $-\phi'(\chi,0)$ in the entire range of the mixed convection parameter ($0 \leq \chi \leq 1$). From these figures, we see that an increase in the wedge angle parameter λ causes enhancements in both the heat and mass transfer, and as a result in the local Nusselt and Sherwood numbers. This phenomenon is true for the entire range of $0 < \chi < 1$. However, it is noticed that the effect of λ on the local Nusselt and the Sherwood numbers is almost negligible.

Figure 4a–c shows the effect of the surface temperature parameter H on the velocity f', temperature θ and the nanoparticles volume fraction ϕ. It is observed that the temperature field increases with an increase in the surface temperature parameter H. This is due to the fact that as the value of H increases, radiation absorption in the boundary layer increases, causing the temperature to increase. In addition, as H increases, both the fluid velocity and the nanoparticles volume fraction increase.

Figure 5a, b illustrates the effect of the surface temperature parameter H on the values of the local Nusselt and the Sherwood numbers in the entire range of the mixed convection parameter $0 \leq \chi \leq 1$, respectively. It can be observed from these figures that the values of

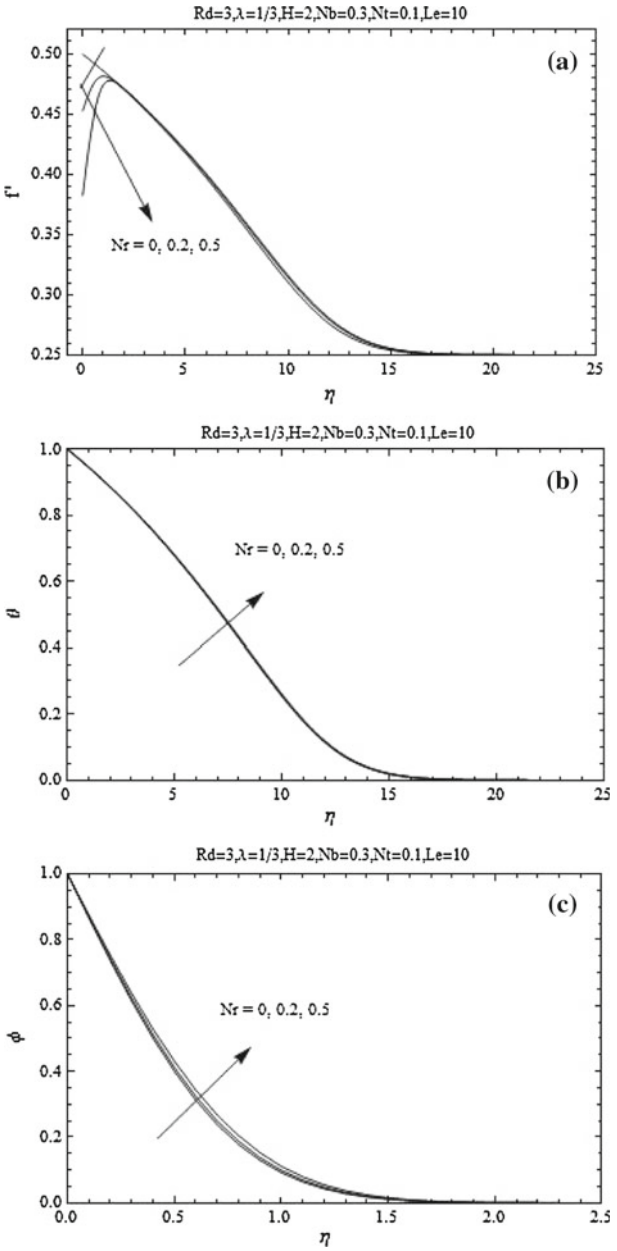

Fig. 6 **a** Effect of Nr on the velocity profiles. **b** Effect of Nr on the temperature profiles. **c** Effect of Nr on the volume fraction profiles

both the local Nusselt and the Sherwood numbers increase as the value of H increases: This is true in the entire range $0 < \chi < 1$. However, the effect of H is almost negligible on the local Sherwood number, but more pronounced with the local Nusselt number.

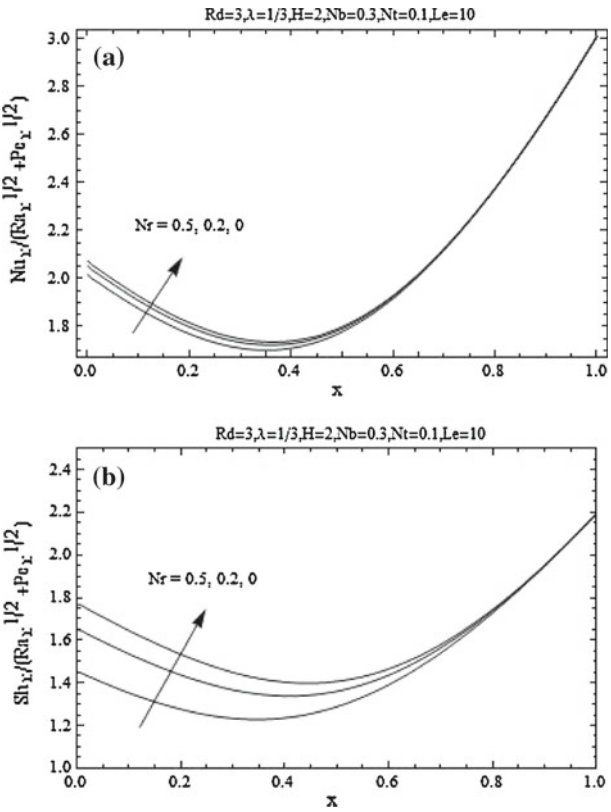

Fig. 7 **a** Effect of Nr on the local Nusselt number. **b** Effect of Nr on the local Sherwood number

Figure 6a–c shows the effects of the buoyancy ratio parameter Nr on the velocity f', the temperature θ and the nanoparticles volume fraction ϕ, respectively. It is found that an increase in Nr decreases the fluid velocity in the immediate vicinity of the wedge surface. This behavior in the velocity is accompanied by a slight increase in the fluid temperature and in the nanoparticles volume fraction as Nr increases.

Moreover, Fig. 7a, b illustrates the changes in the local Nusselt number and the local Sherwood number, for the entire range of the mixed convection parameter $0 \leq \chi \leq 1$ for various values of Nr. It is observed that an increase in the buoyancy ratio enhances both the local Nusselt and the Sherwood numbers. However, for $\chi = 1$ (forced convection limit), the flow is uncoupled from the thermal and volume fraction buoyancy effects, and hence, there is no change in the local Nusselt and the Sherwood numbers for all values of Nr. From the definition of χ, it is seen that an increase in the value of the parameter Ra_x/Pe_x causes the mixed convection parameter χ to decrease. Thus, small values of Ra_x/Pe_x correspond to values of χ close to unity, which indicate almost pure forced convection regime. On the other hand, high values of Ra_x/Pe_x correspond to values of χ close to zero, indicating almost pure free convection regime. Furthermore, moderate values of Ra_x/Pe_x represent values of χ between 0 and 1, which correspond to the mixed convection regime. For the forced convection limit ($\chi = 1$), it is clear from Eq. 7 that the velocity in the boundary layer is uniform. However, for smaller values of χ (higher values of Ra_x/Pe_x) at a fixed

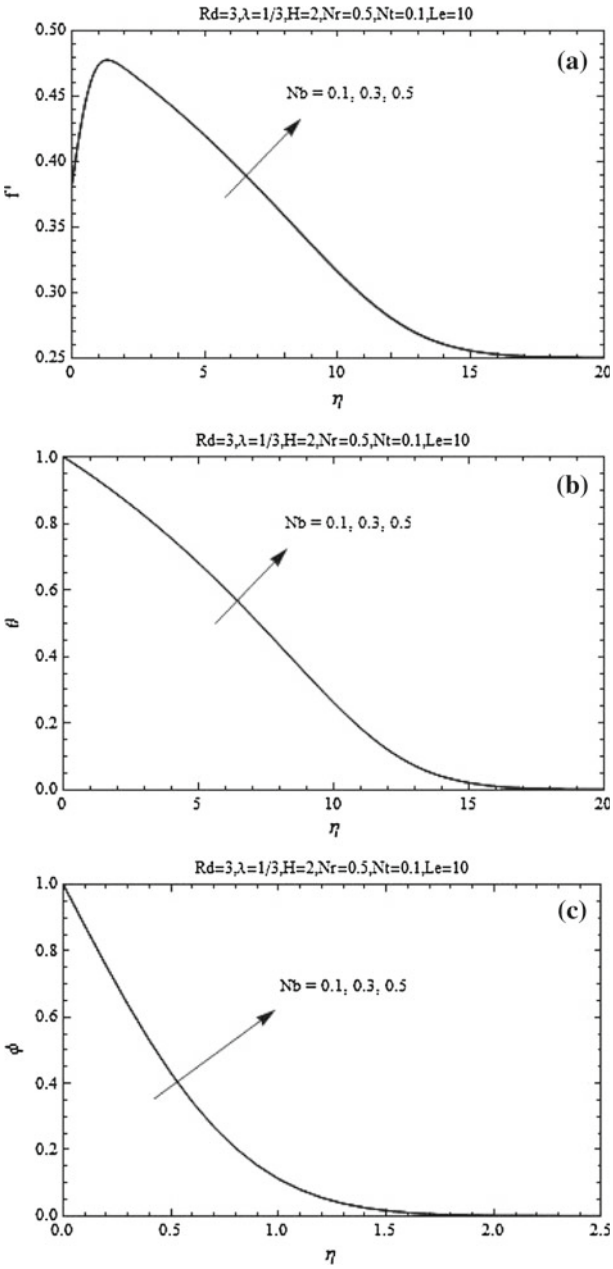

Fig. 8 **a** Effect of *N*b on the velocity profiles. **b** Effect of *N*b on the temperature profiles. **c** Effect of *N*b on the volume fraction profiles

value of *N*r, the buoyancy effects increase. As this occurs, the fluid velocity close to the wall increases for $\chi < 0.5$ due to the buoyancy effect and becomes maximum for $\chi = 0$ (free convection limit). This decrease and increase in the fluid velocity f' as χ decreases from

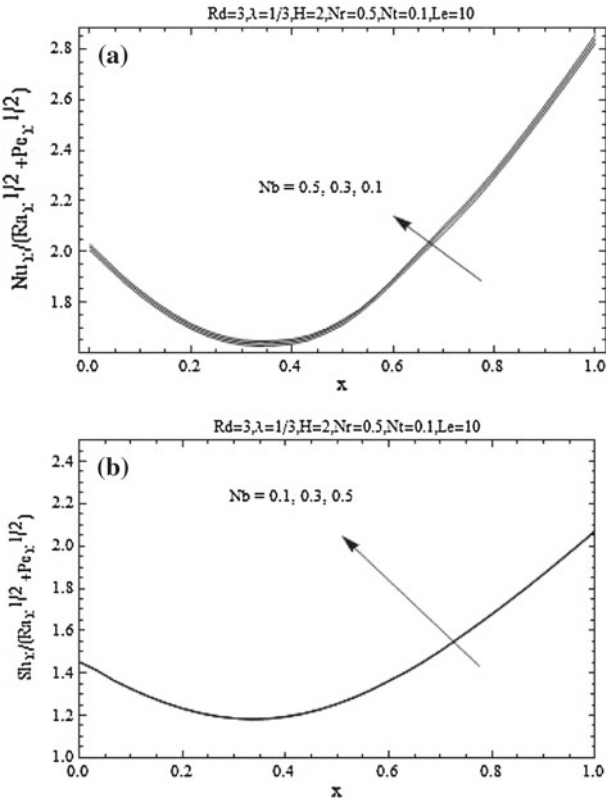

Fig. 9 **a** Effect of Nb on the local Nusselt number. **b** Effect of Nb on the local Sherwood number

unity to zero is accompanied by a respective increase and a decrease in the fluid temperature and concentration. As a result, the local Nusselt and the Sherwood numbers will be affected.

Figure 8a–c presents the effects of an increase in the Brownian motion parameter Nb on the velocity, the temperature and the nanoparticles volume fraction profiles, respectively. It can be seen that as the Brownian motion parameter Nb increases, both the velocity and the temperature increase, especially in the region close to the wedge surface. However, we observe a slight increase in the nanoparticles volume fraction.

In Fig. 9a, b, we present, respectively, the values of the local Nusselt number $-\left(1+(4R_{\mathrm{d}}H^3/3)\right)\theta'(\chi,0)$ and local Sherwood number $-\phi'(\chi,0)$ for different values of the Brownian motion parameter Nb in the entire range of the mixed convection parameter $0 \leq \chi \leq 1$. As observed before, an increase in the Brownian motion parameter Nb is to increase the fluid temperature and the nanoparticles volume fraction. As a result, we see an enhancement in the local Nusselt number or local Sherwood number.

Figure 10a, b displays the typical velocity, the temperature and the nanoparticles volume fraction profiles for various values of the thermophoresis parameter Nt, respectively. An increase in the thermophoresis parameter Nt has the tendency to increase slightly the fluid velocity, the temperature and the nanoparticles volume fraction. Figure 11a–b depicts the influence of the thermophoresis parameter Nt on Nu and Sh, respectively. An increase in the thermophoresis parameter Nt results in an increase in the temperature and the volume

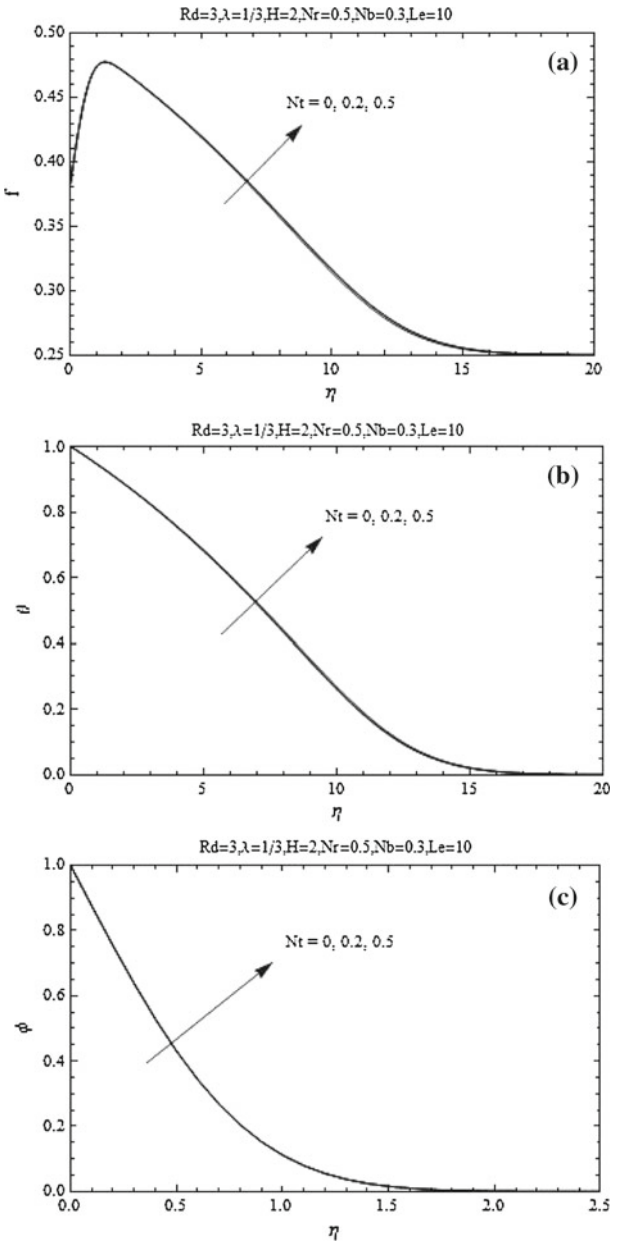

Fig. 10 **a** Effect of Nt on the velocity profiles. **b** Effect of Nt on the temperature profiles. **c** Effect of Nt on the volume fraction profiles

fraction: This causes the value of $-\left(1+(4R_{\mathrm{d}}H^3/3)\right)\theta'(\chi,0)$ to increase and $-\varphi'(\chi,0)$ to decrease.

Figure 12a–c shows the velocity, the temperature and the nanoparticles volume fraction profiles for different values of the Lewis number Le, respectively. It is clearly observed that

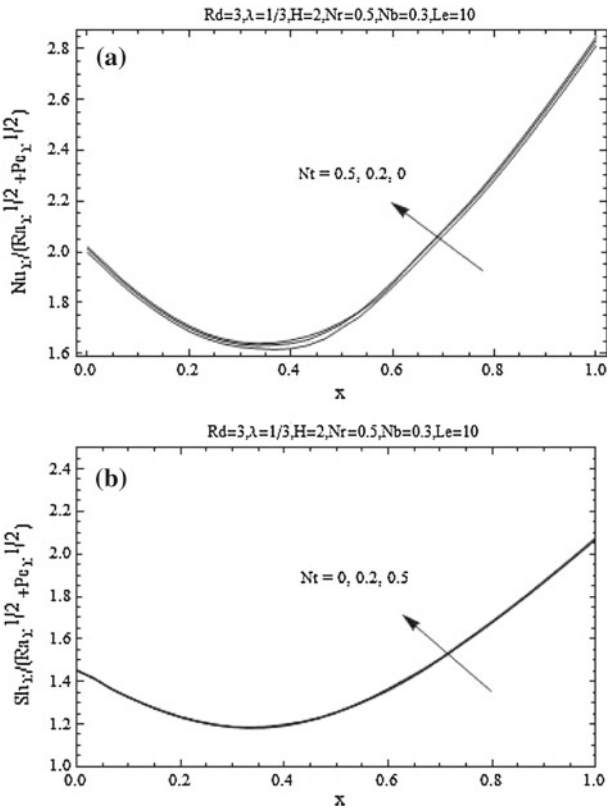

Fig. 11 **a** Effect of Nt on the local Nusselt number. **b** Effect of Nt on the local Sherwood number

the fluid velocity and the temperature increase while the nanoparticles volume fraction and its boundary-layer thickness decrease considerably as the Lewis number Le increases. This results in the enhancement of heat and mass transfer.

Figure 13a, b illustrates the effects of the Lewis number Le on the local Nusselt number and the local Sherwood number for the entire range of the mixed convection parameter $0 \leq \chi \leq 1$, respectively. An increase in the Lewis number Le causes the nanoparticles volume fraction to increase. As a consequence, a reduction in the local Nusselt number and an enhancement in the local Sherwood number are observed.

Figure 14a, b shows, respectively, the effect of the radiation–conduction parameter R_d on the local Nusselt number for the Newtonian fluid and the nanofluids, in the entire range of the mixed convection parameter $0 \leq \chi \leq 1$. It is found that the local Nusselt number and the Sherwood number increase with increasing R_d, for $\chi = 0$ (pure-convection heat transfer). Since the local Nusselt number is proportional to the wall temperature gradient $-\left(1 + (4R_\mathrm{d}H^3/3)\right)\theta'(\chi, 0)$, the local Nusselt number is found to be more sensitive to H and R_d than $-\varphi'(\chi, 0)$, as revealed in Eqs. 12 and 13. Moreover, for $\chi = 1$ (forced convection limit), the flow is uncoupled from the thermal and volume fraction buoyancy effects, and hence, the local Sherwood number does not depend on R_d.

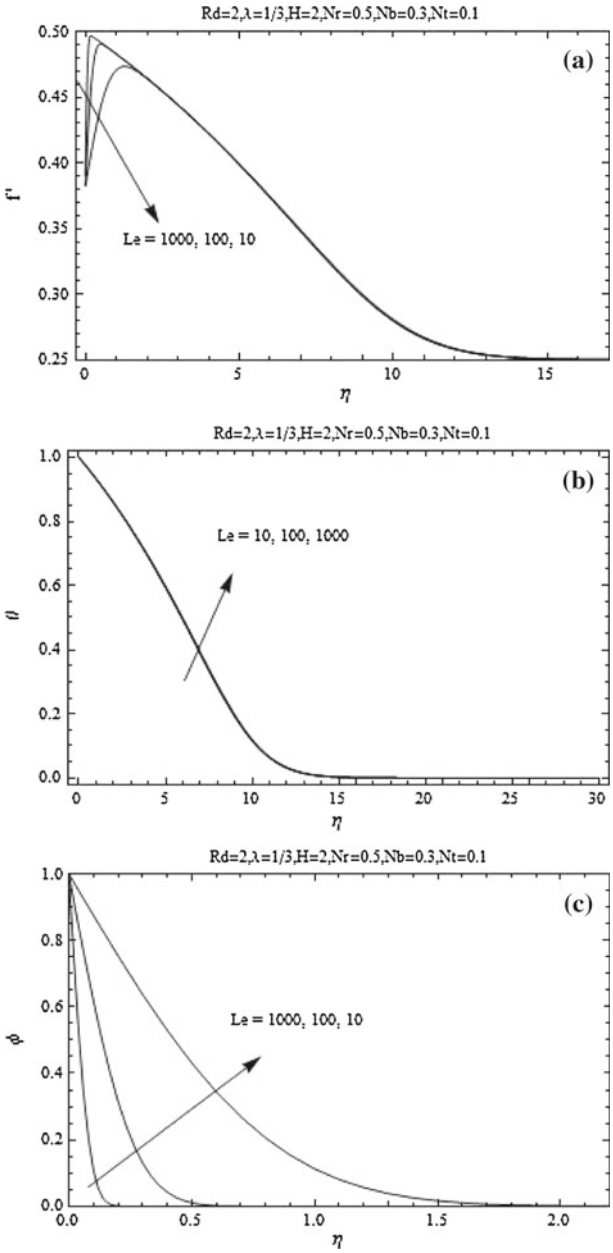

Fig. 12 **a** Effect of *Le* on the velocity profiles. **b** Effect of *Le* on the temperature profiles. **c** Effect of *Le* on the volume fraction profiles

5 Conclusion

Non-similar solution of steady mixed convection flow of a nanofluid adjacent to an isothermal wedge embedded in a saturated porous medium in the presence of thermal radiation

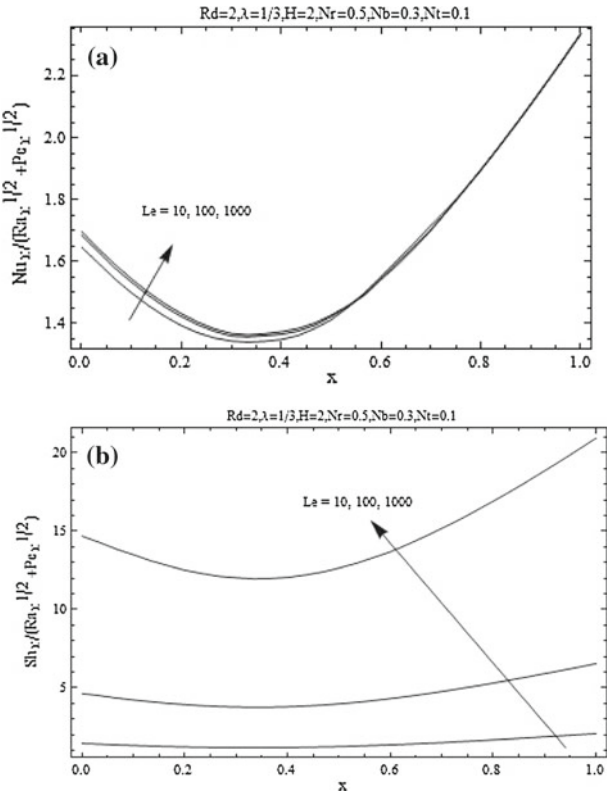

Fig. 13 **a** Effect of Le on the local Nusselt number. **b** Effect of Le on the local Sherwood number

with Rosseland diffusion approximation is investigated. The model used for the nanofluid incorporates the effects of Brownian motion and thermophoresis. The entire regime of mixed convection is included, as the combined convection parameter varies from 0 (pure free convection) to 1 (pure forced convection). The transformed non-linear system of equations is solved by the Keller box method. A comparison between the present (for some special cases) and the previously published results is found to be in very good agreement. The numerical results are presented for the local Nusselt and the Sherwood numbers with several sets of values of the buoyancy ratio, the Brownian motion parameter, the thermophoresis parameter, the wedge angle parameter, the radiation–conduction parameter, the surface temperature parameter and the Lewis number. It was found that the local Nusselt number increases when any of the buoyancy ratio, the Brownian motion, the thermophoresis, the radiation–conduction and the surface temperature parameters, and the Lewis number increases. In addition, the local Sherwood number was increased as the buoyancy ratio, Brownian motion parameter, Lewis number, wedge angle parameter, radiation–conduction parameter or the surface temperature parameter increases. But quite the opposite is seen as the thermophoresis parameter increases. Furthermore, both the local Nusselt and the Sherwood numbers decrease initially, reaching to a minimum for the intermediate value of the mixed convection parameter, and then increase gradually. Moreover, it is observed that the effects of the Lewis number and the thermophoresis parameters are stronger on the local Sherwood number than that on the local Nusselt number. However,

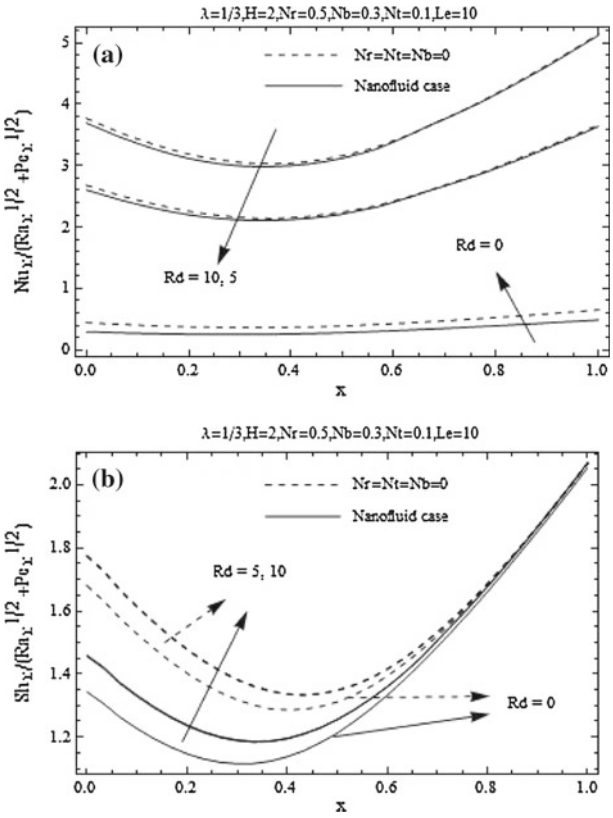

Fig. 14 **a** Effect of *R*d on the local Nusselt number. **b** Effect of *R*d on the local Sherwood number

the effects of the radiation–conduction parameter and the surface temperature parameter are significantly stronger on the local Nusselt number than that on the local Sherwood number.

Acknowledgments The authors appreciate the comments of the reviewers, which have led to definite improvements in the paper.

References

Abu-Nada, E., Oztop, H.F.: Effects of inclination angle on natural convection in enclosures filled with Cu-water nanofluid. Int. J. Heat Fluid Flow **30**, 669–678 (2009)

Alam, M.M., Alim, M.A., Chowdhury, M.M.K.: Free convection from a vertical permeable circular cone with pressure work and non-uniform surface temperature. Nonlinear Anal. Model. Control **12**, 21–32 (2007)

Bakier, A.Y., Rashad, A.M., Mansour, M.A.: Group method analysis of melting effect on MHD mixed convection flow from radiate vertical plate embedded in a saturated porous media. Commun. Nonlinear Sci. Numer. Simul. **14**, 2160–2170 (2009)

Bakier, A.Y.: Thermal radiation effect of mixed convection from vertical surfaces in saturated porous media. Int. Commun. Heat Mass Transf. **28**, 119–126 (2001)

Bejan, A., Dincer, I., Lorente, S., Miguel, A.F., Reis, A.H.: Porous and Complex Flow Structures in Modern Technologies. Springer, New York (2004)

Cebeci, T., Bradshaw, P.: Physical and Computational Aspects of Convective Heat Transfer. 2nd edn. Springer, New York (1984)
Chamkha, A.J., Aly, A.M., Al-Mudhaf, H.: Laminar MHD mixed convection flow of a nanofluid along a stretching permeable surface in the presence of heat generation or absorption effects. Int. J. Microscale Nanoscale Thermal Fluid Transp. Phenom. **2** (2011) Article 3
Chamkha, A.J., Ben-Nakhi, A.: MHD mixed convection—radiation interaction along a permeable surface immersed in a porous medium in the presence of Soret and Dufour effects. Heat Mass Transf. **44**, 845–856 (2008)
Chamkha, A.J., Gorla, R.S.R., Ghodeswar, K.: Non-similar solution for natural convective boundary layer flow over a sphere embedded in a porous medium saturated with a nanofluid. Transp. Porous Media **86**, 13–22 (2011)
Choi, S.U.S.: Enhancing thermal conductivity of fluids with nanoparticle. In: Siginer, D.A., Wang H.P. (eds.), Developments and Applications of Non-Newtonian Flows, ASME FED, vol. **231**/MD 66, pp. 99–105 (1995)
Duangthongsuk, W., Wongwises, S.: Effect of thermophysical properties models on the predicting of the convective heat transfer coefficient for low concentration nanofluid. Int. Commun. Heat Mass Transf. **35**, 1320–1326 (2008)
Gorla, R.S.R., Chamkha, A.J., Rashad, A.M.: Mixed convective boundary layer flow over a vertical wedge embedded in a porous medium saturated with a nanofluid. J. Nanoscale Res. Lett. **6**, 207–216 (2011)
Gorla, R.S.R., EL-Kabeir, S.M.M., Rashad, A.M.: Heat transfer in the boundary layer on a stretching circular cylinder in a nanofluid. J. Thermophys. Heat Transf. **25**, 183–186 (2011)
Hsieh, J.C., Chen, T.S., Armaly, B.F.: Mixed convection along a non-isothermal vertical plate embedded in a porous medium: the entire regime. Int. J. Heat Mass Transf. **36**, 1819–1825 (1993)
Ingham, D.B., Pop, I.: Transport Phenomena in Porous Media, Pergamon, Oxford, (1998), vol. II, (2002)
Kumari, M., Nath, G.: Radiation effect on mixed convection from a horizontal surface in a porous medium. Mech. Res. Commun. **31**, 483–491 (2004)
Nield, D.A., Bejan, A.: Convection in Porous Media. 2nd edn. Springer, New York (2006)
Nield, D.A., Kuznetsov, A.V.: The Cheng-Minkowycz problem for natural convective boundary-layer flow in a porous medium saturated by a nanofluid. Int. J. Heat Mass Transf. **52**, 5792–5795 (2009)
Nield, D.A., Kuznetsov, A.V.: Thermal instability in a porous medium layer saturated by a nanofluid. Int. J. Heat Mass Transf. **52**, 5796–5801 (2009)
Pop, I., Ingham, D.B.: Convective Heat Transfer: Mathematical and computational Modelling of Viscous Fluids and Porous media. Pergamon, Oxford (2001)
Pop, I., Grosan, T., Kumari, M.: Mixed convection along a vertical cone for fluids of any Prandtl number case of constant wall temperature. Int. J. Numer. Methods Heat Fluid Flow **13**, 815–829 (2003)
Takhar, H.S., Chamkha, A.J., Nath, G.: Effect of thermo-physical quantities on the natural convection flow of gases over a vertical cone. Int. J. Eng. Sci. **42**, 243–256 (2004)
Vafai, K.: Handbook of Porous Media. 2nd edn. Taylor & Francis, New York (2005)
Vajravelu, K., Nayfeh, J.: Hydromagnetic convection at a cone and a wedge. Int. Commun. Heat Mass Transf. **19**, 701–710 (1992)
Yih, K.A.: Mixed convection about a cone in a porous medium: the entire regime. Int. Comm. Heat Mass Transf. **26**, 1041–1050 (1999)
Yih, K.A.: Radiation effect on mixed convection over an isothermal wedge in porous media: the entire regime. Heat Transf. Eng. **22**, 26–32 (2001)